

**Motivation:** In the last few years a growing interest in biology has been shifting towards the problem of optimal information extraction from the huge amount of data generated via large scale and high-throughput techniques. One of the most relevant issues has recently become that of correctly and reliably predicting the functions of observed but still functionally undetermined proteins starting from information coming from the network of co-observed proteins of known functions<sup>1</sup>.

**Method:** The method proposed in this article is based on a message passing algorithm known as Belief Propagation<sup>2</sup>, which takes as input the network of proteins physical interactions and a catalog of known proteins functions, and returns the probabilities for each unclassified protein of having one chosen function. The implementation of the algorithm allows for fast on-line analysis, and can be easily generalized to more complex graph topologies taking into account hyper-graphs, *i.e.* complexes of more than two interacting proteins.

**Results:** The benchmark of our method is the *Saccharomices Cerevisiae* protein-protein interaction network (PPI)<sup>3,4</sup> and the validity of our approach is successfully tested against other available techniques<sup>5,6,7</sup>.

**Contact:** leone@isiosf.isi.it, andrea.pagnani@roma1.infn.it

**Keywords:** protein-protein interaction, protein function prediction, message passing algorithms, belief propagation.

## I. INTRODUCTION

The most classical protein function prediction methods are those inferring similarity in function from sequence homologies between proteins listed in databases using programs such as FASTA<sup>8</sup> and BLAST<sup>9</sup>; via comparison with known proteins interactions in similar genomes (the so called *Rosetta Stone Method*<sup>10</sup>); or by phylogenetic analysis<sup>11</sup>. More recently, a new class of methods has been proposed that relies on the available data on the global structure of the PPI networks for a growing number of organisms of completely sequenced genome<sup>3,12,13</sup>. The most complete available on-line data are structured in a graph-like format, with graph sites indexed with protein names and links representing a physical experimentally tested interaction among two proteins. More limited databases on larger protein complexes are also available<sup>14,15</sup>. From the side of functional classification, databases are now available (**MIPS**<sup>24</sup> and **Gene Ontology** among others<sup>25</sup>), that provide a classification of a continuously growing number of proteins, listing them in different functional categories classes with a hierarchical-like organization. Among the presently available methods that try to exploit the global PPI network structure to infer yet unknown functions for unclassified proteins whose interactions with the rest of the graph are at least partially known, there are the so called *Neighboring Counting Method*<sup>16</sup>, the  $\chi^2$  *Method*<sup>17</sup>, the Bayesian approaches<sup>5,6</sup>, the *Redundancy Method*<sup>18</sup> and a more recent Monte Carlo Simulated Annealing (SA) approach<sup>7</sup>.

## II. METHODS

Let us name  $\mathcal{G}$  a PPI graph, with set of vertexes  $V = \{1, \dots, N\}$  representing the observed proteins, each protein name being assigned a numerical value from 1 to  $N$ . Let us also define a mapping between the set of all observed functions and the numbered set  $\mathcal{F} = \{1, \dots, F\}$ . Each protein  $i$  belonging to  $V$  can then be characterized via a discrete variable  $X_i$  that can take values  $f \in \mathcal{F}$ . One would like to compute the probability  $P_i(f) = Pr(X_i = f)$  for each protein to have a given function  $f$  given the functions assigned to the proteins in the rest of the graph. The method is based on the definition of a score function  $E$  on the PPI graph (see eq. (1)), that counts the number of all common predicted functions among neighboring proteins of the graph over all interactions. In addition to this, a certain fraction of the proteins is already classified, which means that there exists a subset  $A \subset V$  of vertexes with at least one function belonging to  $\mathcal{F}$  attached to it (see fig.(1) **(a)** for an example of a graph portion). The effect of the already classified proteins with a given function in the neighborhood of protein  $i$  on the PPI network is taken into account as an external field acting on  $i$  and proportional to the number of the neighbors belonging to  $A$  with that given function. From this score function a variational potential (called Gibbs potential) can be defined that measures the distance between the true unknown function probabilities and a trial estimation of them. The values of the best estimated probabilities are found extremizing the Gibbs potential<sup>2,19</sup>. The Gibbs potential extremizing equations used in this work are commonly known under the name of *Belief Propagation* (BP) equations and can be easily found via a procedure called *Cavity Method*<sup>20</sup>. We have solved the BP equations both for the probabilities of completely

unclassified proteins belonging to  $V \setminus A$  and for the more complete model where we let a protein belonging to  $A$  the possibility of having other yet unknown functions. The modifications to be applied to the method are technical minor so that they will not be described here. Given a choice of initial conditions on probability functions  $\{P_i(X_i)\}_{i=1,\dots,N}$  and a choice of the score function  $E$ , the algorithm calculates the stationary probabilities whose values extremize the resulting Gibbs potential. The potential in general depends on one free real parameter  $\beta$  that plays the role of an inverse temperature and weights the possibility of allowing functional assignments that do not exactly maximize the score, but could still be possible due to their large degeneracy: at low enough values of  $\beta$  (high temperature) almost any function assignment to proteins in  $V \setminus A$  gives an equivalent value of the potential. In this region the system is said to be in a “paramagnetic phase”. Every functional assignment is therefore accepted and the algorithm is not predictive. After a certain critical value  $\beta_c$  the shape of the Gibbs potential changes: only some values of the probability functions extremize it. Augmenting  $\beta$ , the algorithm tends to weight more and more those functional assignments that exactly maximize the score. Strictly at zero temperature ( $\beta \rightarrow \infty$ ) only the score maximizing functional assignments survive with non zero probability. Given sets  $V$ ,  $A$  and  $V \setminus A$ , the PPI graph  $\mathcal{G}$ , the graph of unclassified proteins  $\mathcal{U} \subset \mathcal{G}$  and the set of observed function  $\mathcal{F}$ , a score function can be defined following Vazquez et al.<sup>7</sup> as

$$E[\{X_i\}_{i=1}^N] = - \sum_{ij} J_{ij} \delta(X_i; X_j) - \sum_i h_i(X_i) \quad (1)$$

where  $J_{ij}$  is the adjacency matrix of  $\mathcal{U}$  ( $J_{ij} = 1$  if  $i$  and  $j \in V \setminus A$  and they interact with each other).  $\delta(\sigma; \tau)$  is the Kronecker delta function measured between functions  $\sigma$  and  $\tau$  assigned to the neighboring proteins and  $h_i(\tau)$  is an external field that counts the number of classified neighbors of protein  $i$  in the original graph  $\mathcal{G}$  that have at least function  $\tau$ . The Gibbs potential can then be calculated as a variational way to compute the quantity

$$F = -\frac{1}{\beta N} \log \left( \sum_{\{X_i\}_{i=1,\dots,N}} e^{-\beta E[\{X_i\}_{i=1,\dots,N}]} \right) \quad (2)$$

called free-energy of the system, a fundamental quantity than in statistical physics counts the logarithm of the sum of all the weights of the probabilities each configuration of the variables in the systems appear with. Configurations with a largest statistical weight can then be calculated as those maximizing this potential function. Using the message passing approach<sup>2,20</sup> under the assumption that correlations are low enough in the graph so that one can write  $P_{ij}(X_i, X_j) \propto P_i(X_i)P_j(X_j)$  if proteins  $i$  and  $j$  are chosen at random, one can calculate each  $P_j(X_j)$  as product of conditional probabilities contributions  $M_{i \rightarrow j}(X_j)$  incoming to  $j$  from all neighbors of protein  $j$ , conditional to the fact that  $j$  has function  $X_j$ :

$$P_j(X_j) \propto \prod_{i \in I(j)} M_{i \rightarrow j}(X_j) = e^{\beta \sum_{i \in I(j)} u_{i \rightarrow j}(X_j)} \quad (3)$$

where  $I(j) \subset V \setminus A$  denotes the set of unclassified neighbors of  $j$  and  $u_{i \rightarrow j}(\sigma)$  is a “message” that represents the field in direction  $\sigma \in \mathcal{F}$  acting on protein  $j$  due to the presence of protein  $i$  when protein  $j$  has function  $\sigma$ . Equations for the message functions can be solved iteratively as fixed points of the system of equations

$$M_{i \rightarrow j}(\sigma) = \sum_{\tau=1}^F \left( \prod_{l \in I(i) \setminus j} M_{l \rightarrow i}(\tau) \right) e^{\beta J_{ij} \delta(\sigma; \tau) + \beta h_i(\tau)} \quad (4)$$

one for each link of  $\mathcal{U}$ , for both directions in the graph. Self consistent BP equations can be rewritten in terms of messages  $u$ 's. The ones explicitly used in our algorithm are shown in the following:

$$u_{i \rightarrow j}(\sigma) = \frac{1}{\beta} \log \left( \frac{A(\beta; \vec{T}_{i \rightarrow j}^1(\sigma))}{A(\beta; \vec{T}_{i \rightarrow j}^2)} \right) \quad (5)$$

where

$$\left\{ \begin{array}{l} A(\beta; \vec{T}_{i \rightarrow j}) = \sum_{\tau=1}^F e^{\beta T_{i \rightarrow j}^\tau} \\ \vec{T}_{i \rightarrow j}^{1, \tau}(\sigma) = h_i(\tau) + \sum_{l \in I(i) \setminus j} u_{l \rightarrow i}(\tau) \\ \quad \text{if } \sigma \neq \tau \\ \quad \text{or } h_i(\tau) + \sum_{l \in I(i) \setminus j} u_{l \rightarrow i}(\tau) + 1 \\ \quad \text{if } \sigma = \tau \\ \vec{T}_{i \rightarrow j}^{2, \tau} = h_i(\tau) + \sum_{l \in I(i) \setminus j} u_{l \rightarrow i}(\tau) \end{array} \right.$$

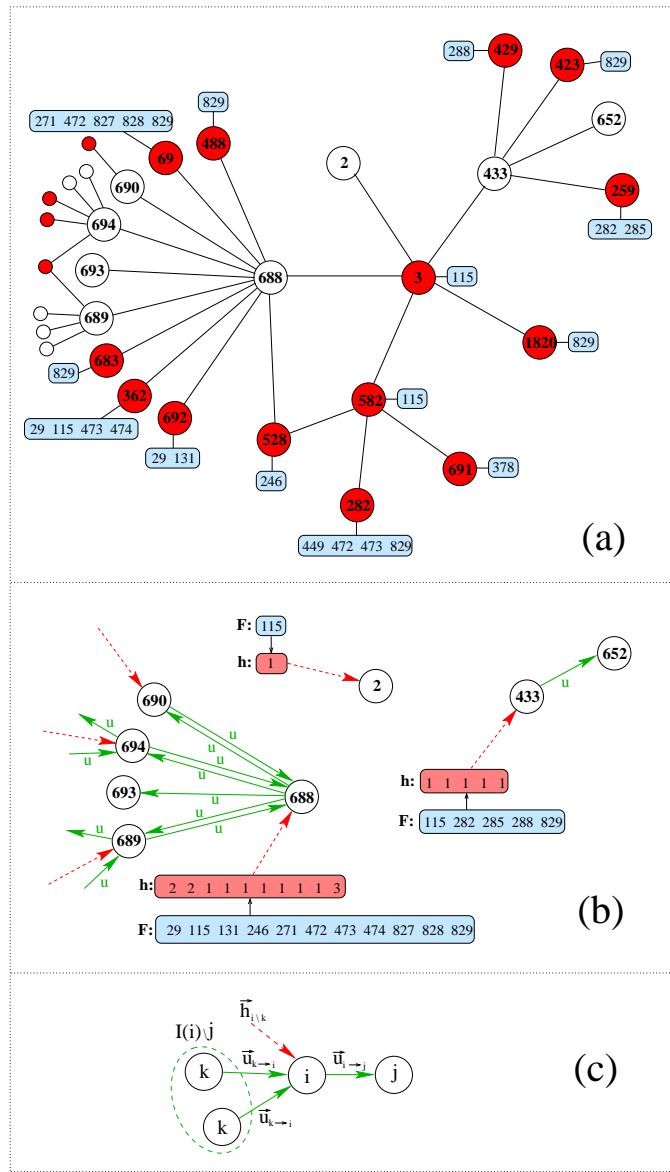


FIG. 1: From  $\mathcal{G}$  to the BP equations: fig.(a) shows a small fraction of  $\mathbf{U}$  network  $\mathcal{G}$ . Circles represent proteins with their numerical ID used by the algorithm. Classified proteins are filled, while unclassified ones are left white. Each classified protein has a series of functions whose numerical values  $\in \mathcal{F}$  are written in boxes. In (b) only the corresponding part of the  $\mathcal{U}$  subgraph has been drawn. Dotted arrows represent external fields acting on the unclassified proteins and are vectors whose non zero components are defined in the Lower boxes. For each protein in  $\mathcal{U}$ , they count the number of classified neighbors having a given function. Upper boxes are sets of all functions of all classified proteins neighboring a given unclassified one. Thick arrows represent “messages” among unclassified proteins according to eq. (4). Notice how  $\mathcal{U}$  is significantly less connected than  $\mathcal{G}$  and often divides in smaller connected components. (c) Is a more detailed representation of the message passing between proteins  $i$  and  $j$ , in direction  $i \rightarrow j$ .

The BP algorithm has been written in terms of that equation and solved at any  $\beta$  with a population dynamic technique<sup>20</sup>. In general, all previously described quantities depend on the inverse temperature  $\beta$ . Eq. (3) turns out to be a good approximation of the solution of the problem of finding the probabilities for configurations maximizing (2). A pictorial view of the iteration procedure is shown in fig (1)(c).

$\mathcal{G}$		$\mathcal{U}$	
cs	noc	cs	noc
2	114	1	248
3	30	2	40
4	23	3	8
5	6	4	7
6	4	5	1
7	1	6	1
8	4	7	1
11	1	14	1
13	1	17	1
1299	1	27	1

TABLE I: Cluster size (cs) and number of clusters (noc) for both the original graph  $\mathcal{G}$  (the two leftmost columns) and the graph of the unknow proteins  $\mathcal{U}$  (the two rightmost columns). Note the giant component of 1299 sites for the  $\mathcal{G}$  graph.

### III. DATA AND GRAPH ANALYSIS

As benchmarks for the method, we have used two yeast *Saccharomyces Cerevisiae* PPI graphs<sup>3,4</sup>, referred in the following as **U** and **D** respectively. The functional categories set  $\mathcal{F}$  was extracted from the MIPS database. The **U** network contains  $N = 1826$  proteins out of which 1370 belong to  $A$ , while the remaining 456 are unclassified or have an unclear MIPS classification; and  $M = 2238$  pairwise interactions. The **D** network contains  $N = 4713$  proteins out of which 3303 belong to  $A$  and 1410 are unclassified; and  $M = 14846$  interactions. Different choices of functional categories sets  $\mathcal{F}$  are possible in the MIPS database, depending on the level of the coarse-grained specification of the hierarchical classification scheme. We used the latest publicly available finest classification scheme retrieving  $F = 165$  functional categories present **U** and  $F = 176$  in **D**, but experiments were run also on the most coarse-grained classification scheme. Results are available upon request.

The PPI graph consists of a giant component of 1299 sites (990 classified), and the rest of the sites are grouped into 184 smaller isolated components of at most 13 sites. We have also analyzed the structure of the  $V \setminus A$  graph which turns of 456 sites, grouped in 309 clusters of size at most 27. Each cluster in  $V \setminus A$  can be considered as an isolated *functional island* of the graph surrounded by external fields as displayed in the last picture of the main body of the paper. More details on the cluster composition of both  $\mathcal{G}$  and  $\mathcal{U}$  for the **U** PPI network are shown in Table I. One may wonder if these clusters are more than a topological feature of our model, but reflect also a more interesting *functional segregation*. In other words one is interested to understand in quantitative terms how different clusters in  $V \setminus A$  label different functional areas in our graphs. To this aim we measured inter-cluster and intra-cluster functional overlaps as in eqs. (6) and (7) Both observables take value in the interval (0,1) and give a measure of the functional similarity of clusters (higher values indicate higher similarity). The emerging scenario shows clear signs of segregation since the intra-cluster overlap distributions has support in the interval (0,0.1) while the inter-cluster distribution has support in the whole interval (0,1). This test can be interpreted as a coherence test on the graph itself, and also on the working hypothesis of our method, since segregation is tacitly assumed in the functional form of score function where only first neighbors interactions on the graph are taken into account. Let us define the notion of intra and inter cluster functional overlap as

$$O_i = \frac{1}{N_i^2} \sum_{l,k \in \mathcal{C}_i} \frac{\phi(s_l, s_k)}{\Phi(\mathcal{C}_i)} \quad (6)$$

$$o_{ij} = \frac{1}{N_i N_j} \sum_{l \in \mathcal{C}_i} \sum_{k \in \mathcal{C}_j} \frac{\phi(s_l, s_k)}{\Phi(\mathcal{C}_i \cup \mathcal{C}_j)} \quad i \neq j \quad (7)$$

where index  $i$  labels the different clusters  $\mathcal{C}_i$  and run between 1 and the total number of clusters  $C$ ,  $N_i$  is the number of site in cluster  $\mathcal{C}_i$ ,  $\phi(s_l, s_k)$  counts the number of function that site  $l$  and  $j$  have in common, and  $\Phi(\mathcal{C}_i)$  is the number of different functions acting onto cluster  $\mathcal{C}_i$ , while  $\Phi(\mathcal{C}_i \cup \mathcal{C}_j)$  is the number of different functions acting onto the union set  $\mathcal{C}_i \cup \mathcal{C}_j$ . It is interesting to note that according to Eqs. 6, 7 both  $o_i$  and  $O_{ij}$  have take real values in the interval

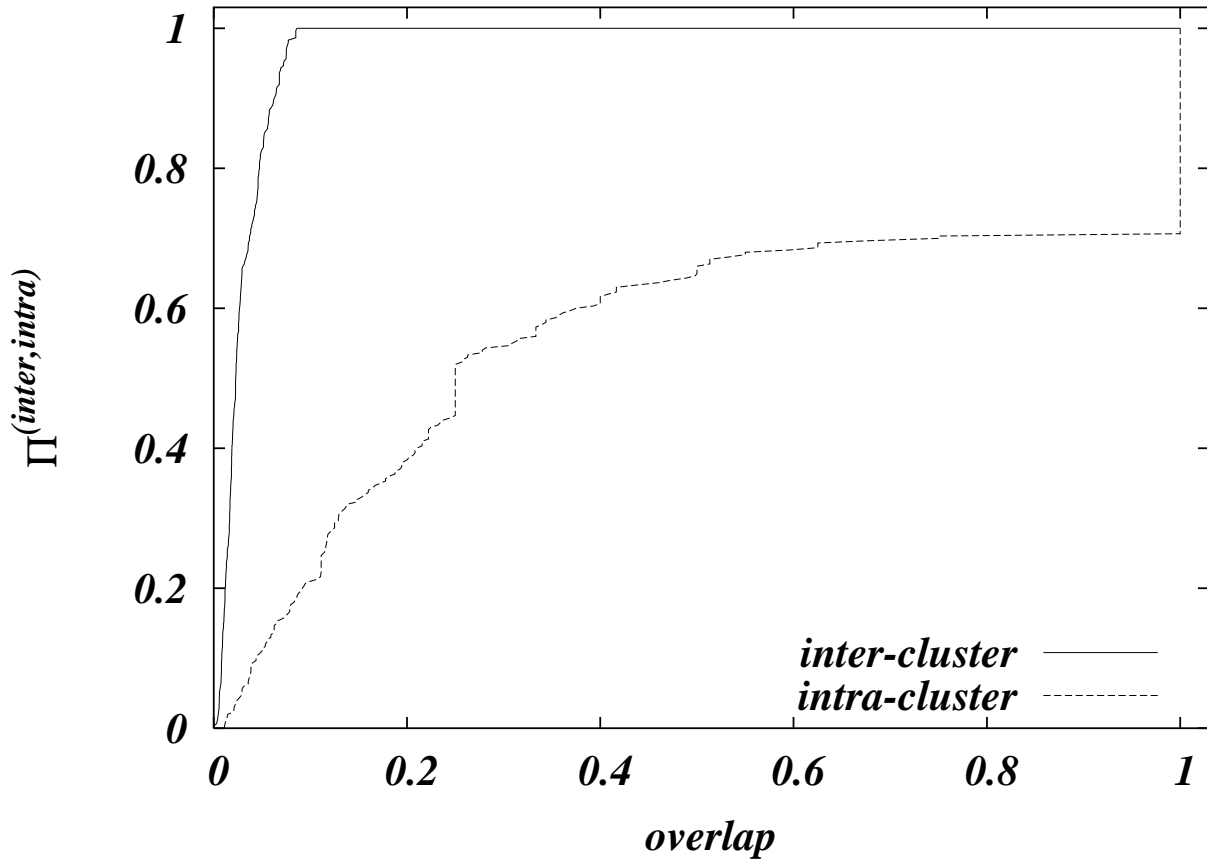


FIG. 2: Cumulative probability distribution of intra/inter-cluster functional overlap as defined in Eqs. 6, 7 for the  $\mathbf{U}\mathcal{U}$  graph . Since the intra-cluster overlap turns out to be always lower than 0.085, the intra-cluster cumulative probability distribution (solid line) saturates to 1 above this value. The inter-cluster overlap instead shows clear sign of segregation. Note that the sudden jump at 1 for the dashed line is due to a significative fraction of clusters (84 out of 309) with functional overlap strictly equal to one.

(0,1). We can consider probability densities of the two variables  $O_i$  and  $o_{ij}$  as

$$P^{(\text{intra})}(O) = \frac{1}{N} \sum_{i=1}^C \delta(O, O_i) \quad (8)$$

$$P^{(\text{inter})}(o) = \frac{1}{N(N-1)} \sum_{1 \leq i < j \leq C} \delta(o, o_{ij}) \quad (9)$$

where  $\delta(a, b)$  is the Kronecker delta function equal to 1 when  $a = b$  and zero otherwise. It is interesting at this point to compare the average intracenter overlap  $\langle O \rangle = 0.440673$  with the average intercenter overlap  $\langle o \rangle = 0.0294147$  which is a factor 15 smaller and that can be taken as a quantitative measure of the functional segregation on the PPI graph.

We define then the cumulative distribution functions as

$$\Pi^{(\text{intra})}(O) = \int_0^O P^{(\text{intra})}(x) dx \quad (10)$$

$$\Pi^{(\text{inter})}(o) = \int_0^o P^{(\text{inter})}(x) dx . \quad (11)$$

The two cumulative functions are displayed in Fig.2. The algorithm can be run separately and in parallel on all connected components of  $\mathcal{U}$ , because there no exchange of information between them. Equivalently speaking, the score function can be written as a sum over all components  $c$  of separated scores:  $E = \sum_c E_c(\{X_i\}_{i \in c})$ .

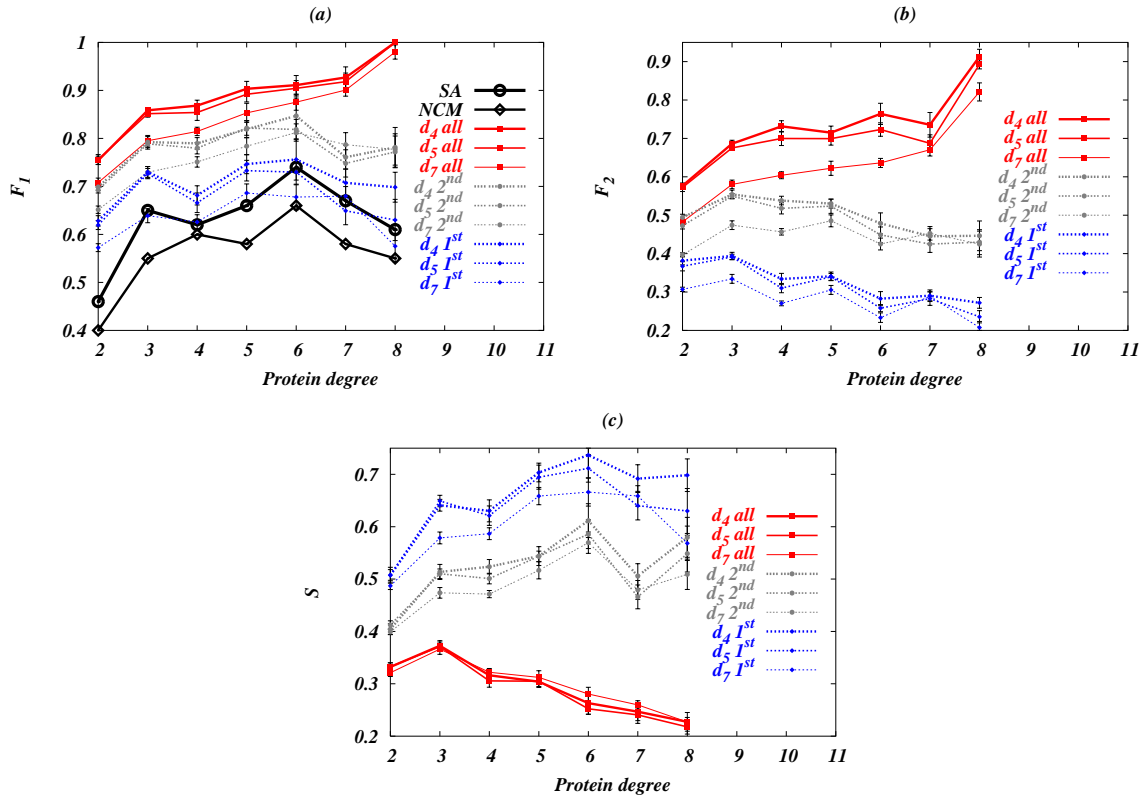


FIG. 3: (a)  $F_1$ , (b)  $F_2$  and (c) Sharpness versus protein degree for different  $\mathcal{U}$  dilutions, as described in the text. Results are displayed for three dilution levels  $d_4 = 0.4$ ,  $d_5 = 0.5$ ,  $d_7 = 0.7$ . Dotted lines are results considering only functions of higher probabilities (1<sup>st</sup> best rank). Dotted-dashed lines are results considering both best and second best ranks. Thick lines consider all non background noise ranks. SA and NCM are the Simulated Annealing and the Neighboring Counting Method results for dilution  $d = 0.4$ . Notice that a low value of Sharpness does not necessarily indicate a poor performance of the algorithm. It could also be due to the fact that indeed many functions have not been observed also in already classified proteins and therefore the catalogs are incomplete not only for proteins in  $\mathcal{U}$ , but on all  $\mathcal{G}$ .

#### IV. RESULTS

We have run our algorithm solving eqs. (3) and (4) at several values of  $\beta > \beta_c$  and for different choices of initial conditions of populations  $\{P_i(X_i)\}_{i=1,\dots,N}$ . Results are always very stable with respect to initial conditions. Instead of maximizing the Gibbs potential directly at zero temperature we have worked at finite  $\beta$  because we were interested also in predicting functional assignments that could be biologically allowed although not strictly maximizing the score function (1). Above  $\beta_c$ , the function probabilities for each protein converge on a set of values organized in hierarchies. The probability values are  $\beta$ -dependent, but not so the hierarchical structure (see fig (5) for an example). All results presented in the following are therefore taken at one given high value of  $\beta$  ( $\beta = 2$  for the DIP PPI graph and  $\beta = 10$  for the  $\mathcal{U}$  PPI graph). For any protein  $i$  and the connected component  $c$   $i$  belongs to, we have filtered out all background noise probability values for functions that are not present in  $c$  and still have a non zero contributions due to the form of eq. (3). We have then collected and ranked the remaining functional probabilities, following their emerging hierarchical structure. A list of predicted functions for all the unclassified proteins in the  $\mathcal{U}$  PPI network using MIPS 2003 functional categories catalog is presented in the **Supplementary Table**. The rank division is explained in fig.(5). In order to probe the reliability of our algorithm, we have followed the standard procedures of Vazquez et al.<sup>7</sup>: starting from  $\mathcal{G}$  and a corresponding MIPS functional annotation, we disregarded the functions of a given fraction  $d$  of classified proteins and considered them as unclassified. We have called  $d$  “dilution” of  $\mathcal{G}$ . If a previously classified protein is considered unclassified we say it has been “whitened”. With this procedure one obtains a new larger graph  $\mathcal{U}_d$  of unclassified proteins, where the algorithm can be run and its ability of finding again the erased functions can be tested. This testing procedure is very similar but more stringent than the *Leave One-Out Method*<sup>5</sup>, because it assumes as unclassified an extensive fraction of proteins in the graph instead of only one each time. We repeated the procedure for both PPI networks. Results for a set of performance parameters are presented

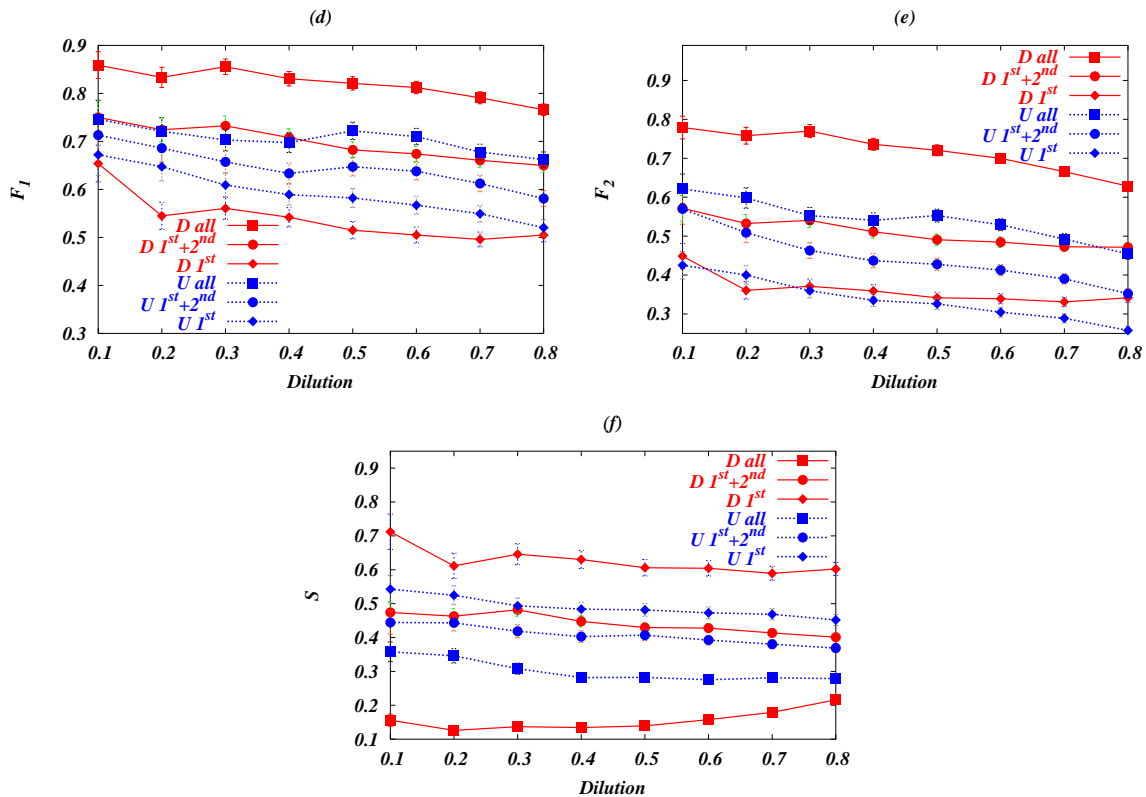


FIG. 4: **(d)**  $F_1$ , **(e)**  $F_2$  and **(f)** Sharpness versus dilution, averaged over all the PPI network and over  $n = 10$  random dilution realizations. Thick lines are results for the **D** network, dotted for **U**. For each network we have again considered 1<sup>st</sup> best, 1<sup>st</sup> and 2<sup>nd</sup> best and all non noise ranks results. The different spacing between lines comparing the two networks reflect their different topological structure. Proteins to be whitened were chosen randomly in  $A$ . The procedure was repeated  $n = 10$  times (Larger  $n$  datasets can be easily produced, but data are already very stable for  $n = 10$ ) for each  $d$ , and the results averaged. We disregarded as statistically non significant the few observed proteins with  $k > 8$ .

in fig. (3) as a function of protein degrees for some fixed dilution values: **Fig.(a):Reliability**. We have defined as a first reliability parameter  $F_1$  the fraction of whitened proteins for which the algorithm predicts correctly *at least one* function. **Fig.(b)** measures a second reliability parameter  $F_2$ , defined as the fraction of correctly predicted functions out of all functions a whitened protein has on the original graph  $\mathcal{G}$ . This test is more stringent because it checks the ability of the algorithm of predicting not only one function, but as many as it can. It is worth noticing that under the  $F_2$  test the method still performs very well when all non background noise ranks are considered. The *legenda* is the same as in picture (a). **(Fig.c): Sharpness**.  $S$  measures the precision of the method and it is defined as the fraction of the number of correctly predicted functions over the number of all predicted ones. It is intuitive that the sharpness decreases with the number probability levels (ranks) one accepts as significant. For whitened proteins of degree 5, for instance, on average only 31% of predicted functions belong to the set of already known erased ones, while in the case of best ranks only, this percentage raises to 65%-70%. In case one allows the algorithm to predict still experimentally unobserved functions also on the classified proteins in  $\mathcal{G}$ , the sharpness still decreases. Results as a function of network dilution. are presented in fig. (4) When (see fig. (3).(a)) a direct comparison with other methods on the same  $\mathcal{G}$  and MIPS catalog was possible, results of our method were systematically better than both the Neighboring Counting Method and the SA. Performance further improves if we consider non only highest rank predictions, but all significant non background noise probabilities. Together with the other available methods, BP performs worse in predicting functions on leaves of the PPI graph, i.e. on whitened proteins with only one neighbor. Nevertheless, even in this case we observed better reliability results.

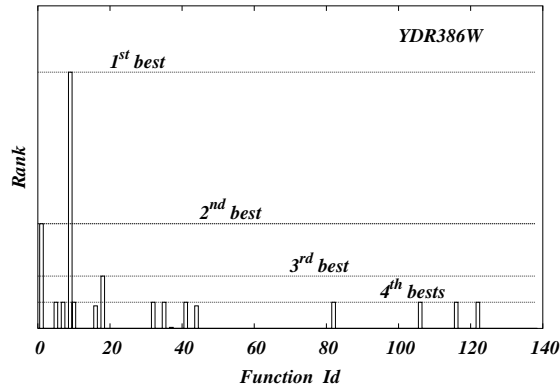


FIG. 5: Example of predicted probabilities ranks for protein YDR386W in the MIPS catalog and for the  $\mathcal{U}$  PPI network. In this example, out of all possible 140 functions only the ones with a vertical bar have non background noise probabilities. Bars heights (*ranks*) are proportional to the logarithm of the probability of having a given function for all the functions ordered on the horizontal axis.

## V. DISCUSSION

**Hierarchical probabilities structure:** Let consider as a simple example a protein  $i$  surrounded by 3 classified neighbors, two having function  $\sigma$  and one having function  $\tau$ . according to (3), in the zero temperature ( $\beta \rightarrow \infty$ ) limit one has  $P_i(\sigma) = 1$  and  $P_i(\tau) = 0$  together with all other function probabilities. However, if the interaction between protein  $i$  and the one neighbor with function  $\tau$  is correct, a biologically more sound functional assignment would be that of giving to protein  $i$  both functions. Working at finite  $\beta$  one can see again from (3) that a non zero value of  $P_i(\tau)$  is also found. The numerical value will continuously depend of  $\beta$ . The hierarchy of the values of the predicted probabilities turns out to be nevertheless very stable after crossing the critical point  $\beta_c$ . One example of probabilities at convergence at a given  $\beta$  and for a randomly chosen protein is given in fig. (5).

**Extension to the algorithm from the unclassified proteins graph  $\mathcal{U}$  only to all proteins in  $\mathcal{G}$ :** Looking at four subsequent versions MIPS databases releases (2001, 2002, 2003 and 2004 respectively), one can see that new functions are progressively assigned to already classified proteins too, so that an inference procedure that allows for this possibility is in principle more complete. However, this procedure can lead to a spreading in the values of inferred probabilities, loosing in Sharpness. Indeed, we tested the performance of our algorithms in both the general and the restricted case, without noticing any significant difference in performance. In fact, since  $\mathcal{G}$  is significantly more connected than  $\mathcal{U}$  the algorithm is significantly slower in reaching convergence of the probability values (It still requires one single run, being therefore faster than the SA approach). Nevertheless, the possibility that the more general case would work significantly better under the definition of a more refined score function, or with a more complete and reliable PPI network, or with the extension of the method to multi-body interactions taking into consideration larger protein complexes cannot be ruled out. Results shown in the body of the text have been limited for clarity to the restricted case where inference is measured only on proteins  $\in V \setminus A$  and for the 2002 and 2003 MIPS catalogs, in order to compare them with results already present in the literature. The same algorithm could be run on the latest 2004 MIPS catalog release with no effort.

**Comparison with other available methods.** Differently from SA<sup>7</sup>, BP algorithm allows to compute directly and in a single run all probabilities  $P_i(f)$  for a given protein  $i$  to be assigned a function  $f$ . This is an advantage with respect to the SA approach, where the output of a single run is one configuration only out of a mutually exclusive set, and in order to obtain trustful probabilities one should average over a large number of SA runs. Moreover, provided one can trust the numerical BP results hierarchies at convergence, some non ground state configurations that could have a biological sound interpretation (see Methods for details) are captured in the BP approach in a hierarchical way, while are missed by SA unless one had time to run a number of cooling experiments of the order of  $10^6$  (Compare with the  $10^2$  runs reported in Vazquez et al.<sup>7</sup>). Differently from Kasif et al.<sup>6</sup>, our version of BP naturally converges and does not therefore need iterations truncation. The connection of computed probability values with the real unknown ones can be made only at convergence of the BP iteration equations, and it is not clear how to interpret the probability values after only a limited number (two in Kasif et al.<sup>6</sup>) of iteration steps, when one could still be in the middle of a transient still heavily dependent on initial conditions. Moreover, truncating the iteration after a small number of steps means disregarding propagation of information coming from distant regions of the network, which is the spirit of any message passing algorithm like BP. The method could still in principle work if the most distant message passing



nodes of any chosen node  $i \in V \setminus \mathcal{A}$  were a few neighboring steps away. This turns out to be almost the case for the considered PPI networks, due to high clusterization and function segregation of  $V \setminus \mathcal{A}$ , as described in Methods, but it is not generally true in inference problems. In a second Bayesian approach<sup>5</sup>, a large number of external parameters (one set for each function) has to be estimated before running the Bayesian inference algorithm. Still, the Gibbs potential<sup>5</sup> could in principle be of a more complete form, allowing for the presence of a chemical potential-like terms (one for each function) proportional to the overall number of times one function is present in the graph. However, it is not clear what the reliability of the biological significance of a term of this type, since influence from the classified functions of distant proteins should already be taken into account in the structure of the message passing procedure. Moreover, if the property of functional segregation was true also on the complete (still unknown) PPI network (See Barabasi et al.<sup>21</sup> for some indications that this might be the case), it is not clear why a protein should have a high probability of being classified with a certain function only because a large group of proteins with a very frequent function existed, even if not interacting with the protein under consideration. In addition, our BP method does not require keeping track of single configurations of functions under the iterations, but only directly of probability weights. The algorithm converges to a stable fixed point and does not need the definition of a measuring time window period<sup>15</sup>. Together with the Monte Carlo approach, our algorithm does not need previous estimation of external parameters defining the Gibbs potential, except for the overall tuning inverse temperature  $\beta$ .

**Limitations.** Our method has got of course many limitations. **(1)** The uncertainty over the graph structure, due to the presence of false positive and false negative interactions. The network topology could vary greatly and the network instead of being divided into connected components could be made of essentially only one giant component. The degree distribution of the network could vary, even though some authors suggest there is evidence for a stabilization towards a scale-free like form<sup>21</sup>. Attempts of healing PPI networks errors or missing links are described in the literature<sup>22,23</sup>, together with a general description of a message passing approach to network reconstruction<sup>19</sup>. Our algorithm could be generalized to partially deal in parallel with these problems, considering two sets of dynamical variables  $\{X_i\}$  and  $\{J_{ij}\}$  instead of  $\{X_i\}$  only. Each  $J_{ij}$  could then take values in a discrete set measuring the likelihood of the interaction between proteins  $i$  and  $j$  to be present as a function of reliability of the experimental data and of the predicted functions assigned to the proteins under consideration. The extrapolated set  $\{J_{ij}\}$  could then be taken as a starting point to calculate new function probabilities over the whole graph using again the BP procedure. Extensions of the method in this direction are under study but are not presented in this paper. **(2)** Pairwise interactions in the observed PPI graph could hide a more complex hyper-graph like structure, with more than two proteins interacting through protein complexes. Our algorithm is readily generalizable to these cases, but we have not tried to test it on actual data yet. **(3)** The way the BP algorithm predicts functions on classified proteins is intrinsically different from the way new annotations are listed in the growing catalogs: to the authors understanding, experiments are typically run concentrating on one or a limited number of interesting function, while other functions could be disregarded. The inference algorithms predictions treat all functions in the same way, so frequency of predicted functions could differ significantly from the experimentally observed ones. **(4)** The numerical values of the probabilities can be proved to be correct (for a given score function) only in the case the PPI graph is strictly a tree. This is not the case for the experimental data, where cycles are present. However, we believe that the order of magnitude of the  $P_i(X_i)$  values should be trustful. This approximation is one of the sources of error in the results of fig. (3). **(5)** The PPI graph is usually built as a time and space average of all processes going all within the cell: a given protein classified for instance with functions 1 and 2 could in principle interact with two other proteins at times in the cell cycle and/or in different places. One of the neighboring protein could then take common function 1, while the other could take common function 2, in a perfectly sound configuration. Running the BP algorithm on the averaged graph would however lead to the prediction of both functions on both neighbors. In this way the algorithm would lose predictive power and sharpness, however it would still predict the correct functions with a certain probability whose exact numerical values should again be taken “cum grano salis”, as already said in point (4). **(6)** Different databases information should be merged in a proper way: for instance, the **U** and **D** PPI graphs are significantly different both in overlap and in topological structure (this point is strictly connected with (1)). We have decided to apply the function prediction method to both graphs separately, but in principle it could be used on a merging of different networks that properly weights relative reliability of interaction links. **(7)** The Kronecker delta function defines a binary distance between functions: one link in  $\mathcal{U}$  contributes 1 to the total score only if the interacting proteins have exactly the same function; 0 otherwise. However, The MIPS classification scheme is organized hierarchically: some proteins have very specific functions, while others can be classified only in a more coarse-grained functional categories. The choice of a binary distance is probably appropriate if one considers only functional categories at a given hierarchical level but it seems unsatisfactory for the total classification, where a more complete notion of hierarchical distance between different functional categories would be needed. In particular one would like to have a distance that recognizes as possibly close two neighboring proteins of functions  $\sigma$  and  $\tau$  in the case  $\sigma$  belongs to a very specific functional category, while  $\tau$  belongs only to a broader one that includes the first, but with no further specification. In this paper we have limited the method to the binary distance score function (1), considering only functions at a chosen hierarchical level in the

MIPS catalogs and disregarding all the others. In this way some information on partial knowledge of the functions assigned to a given protein is lost. This limitation becomes particularly dramatic in the case of the use of catalogs that are not organized hierarchically, but in a more complex way such as Gene Ontology. Extensions of this method are under study.

## VI. ACKNOWLEDGEMENTS

The authors would like to thank Paolo Provero for having given us the starting input for this work, together with Riccardo Zecchina for fruitful discussions and critical reading of the manuscript; Alexei Vazquez, Alessandro Flammini and Vittoria Colizza for data and discussions.

- 
- <sup>1</sup> Hodgman, T. C. A historical perspective on gene/protein functional assignment. *Bioinformatics* **16**, 10-15 (2000).
  - <sup>2</sup> Yedidia, J.S., Freeman, W.T. and Weiss, Y. Understanding Belief Propagation and Its Generalizations, Exploring Artificial Intelligence in the New Millennium, ISBN 1558608117, Chap. 8, pp. 239-236, (2003).
  - <sup>3</sup> Uetz, P. et al. A comprehensive analysis of protein-protein interactions in *Saccharomyces cerevisiae*. *Nature* **403**, 623-627 (2000).
  - <sup>4</sup> The Database of Interacting Proteins, <http://dip.doe-mbi.ucla.edu/>
  - <sup>5</sup> Deng, M. et al. Prediction of protein function using protein-protein interaction data, Proceeding of IEEE Computer Society Bioinformatics Conference (2002).
  - <sup>6</sup> Letovsky, S. & Kasif, S. Predicting protein function from protein/protein interaction data: a probabilistic approach, *Bioinformatics* **19** Suppl 1:i197-204 (2003).
  - <sup>7</sup> Vazquez, A, Flammini, A., Maritan, A. & Vespignani, A Global protein function prediction in protein-protein interaction networks. *Nature Biotech.* **21**, 697-700 (2003).
  - <sup>8</sup> Pearson, W. R. & Lipman, D. J. Improved Tools for Biological Sequence Comparison, *PNAS* **85** 2444-2448 (1988).
  - <sup>9</sup> Altschul, S. F. et al. Gapped BLAST and PSI-BLAST: a new generation of protein database search programs, *Nucleic Acids Research* **25** 3389-3402, (1997).
  - <sup>10</sup> Marcotte, E. M. et al. Detecting protein functions and protein-protein interactions from genome sequences, *Science* **285** 751-753, (1999).
  - <sup>11</sup> Marcotte, E. M. et al. A combined algorithm for genome-wide prediction of protein function, *Nature* **402** 83-86, (1999).
  - <sup>12</sup> Ito, T. et al. Toward a protein-protein interaction map of the budding yeast: A comprehensive system to examine two-hybrid interactions in all possible combinations between the yeast proteins. *Proc. Nat. Acad. Sci.* **98**, 4569-1147 (2001).
  - <sup>13</sup> Giot, L. et al. A protein interaction map of *Drosophila melanogaster*, *Science*. **302**(5651) 1727-36 (2003).
  - <sup>14</sup> Gavin A. C. et al. Functional organization of the yeast proteome by systematic analysis of protein complexes, *Nature* **415**, 141-147, (2002).
  - <sup>15</sup> Ho, Y. et. al. Systematic identification of protein complexes in *Saccharomyces Cerevisiæ* by mass spectrometry, *Nature* **415**, 180-183, (2002).
  - <sup>16</sup> Schwikowski, B., Uetz, P. and Fields, S. A network of protein-protein interactions in yeast. *Nature Biotech.* **18**, 1257-1261 (2000).
  - <sup>17</sup> Hishigaki, H., Nakai, K., Ono, T., Tanigami, A., & Tagaki, T. Assessment of prediction accuracy of protein function from protein-protein interaction data. *Yeast* **18**, 523-531 (2001).
  - <sup>18</sup> Samanta, M. P. & Liang, S. Predicting protein functions from redundancies in large-scale protein interaction networks, *Proc. Nat. Acad. Sci.* **100**, 12579-12583, (2003).
  - <sup>19</sup> Yeang, C.-H. & Jaakkola, T. Physical network models and multi-source data integration. In The Seventh Annual International Conference on Research in Computational Molecular Biology, (2003).
  - <sup>20</sup> Mèzard, M. & Parisi G., *Eur. Phys.J. B* **20**:217 (2001).
  - <sup>21</sup> Yook, S. Y., Oltvai, Z. N. & Barabasi, A.-L. Functional and topological characterization of protein interaction networks to be published in *Proteomics* (2003). Also available at URL: <http://www.nd.edu/~networks/papers.htm>
  - <sup>22</sup> Lappe, M. & Holm, L. Unraveling protein interaction networks with near-optimal efficiency, *Nature Biotech.* **22** 1, 98-103 (2004).
  - <sup>23</sup> Jansen, R. et al. A Bayesian Networks Approach for Predicting Protein-Protein Interactions from Genomic Data, *Science* **302** 449-453 (2003).
  - <sup>24</sup> The MIPS Comprehensive Yeast Genome Database (CYGD), <http://mips.gsf.de/proj/yeast/CYGD/db/>.
  - <sup>25</sup> The Gene Ontology Consortium, <http://www.geneontology.org/>